IEEE Access
Multidisciplinary | Rapid Review | Open Access Journal

Received February 29, 2020, accepted March 13, 2020, date of publication March 17, 2020, date of current version March 30, 2020.

Digital Object Identifier 10.1109/ACCESS.2020.2981505

Deep Compressive Single Pixel Imaging by Reordering Hadamard Basis: A Comparative Study

XIAO YU[1], FAN YANG[1], (Member, IEEE), BING GAO[1], JIA RAN[2], AND XIN HUANG[3]

[1]State Key Laboratory of Power Transmission Equipment and System Security and New Technology, School of Electrical Engineering, Chongqing University, Chongqing 400044, China
[2]School of Optoelectronic Engineering, Chongqing University of Posts and Telecommunications, Chongqing 400065, China
[3]School of Automation, Chongqing University of Posts and Telecommunications, Chongqing 400065, China

Corresponding author: Fan Yang (yangfancqu@gmail.com)

This work was supported in part by the National Natural Science Foundation of China under Grant 51777023, in part by the Graduate Scientific Research and Innovation Foundation of Chongqing under Grant CYB17010, and in part by the Science and Technology Research Program of Chongqing Municipal Education Commission under Grant KJQN201900602.

ABSTRACT Single pixel imaging (SPI) combined with compressed sensing techniques can provide solutions for special optical imaging to avoid array detectors and raster scanning. However, the imaging speed should be further improved for real-time SPI and the challenge is to reduce the sampling time and post-processing time. This paper proposes a deep compressive and super-fast single pixel imaging protocol based on reordering Hadamard basis patterns and Fourier domain regularization inversion (FDRI) algorithm. Two reordered Hadamard basis patterns in terms of the improvement in the compressing ratio and reconstruction quality are proposed and compared to other methods. The deterministic Hadamard basis are reordered through their total variation (TV) in ascending order and total wavelet transformed coefficients (TW) in ascending order to have the best performance. Numerical simulation shows that this protocol can reconstruct a 128×128 pixels natural image at the sampling ratio of 5% with the peak-signal-to-noise ratio (PSNR) of 25.56 dB in 0.00039s. Terahertz near-field imaging experiment also verifies the proposed protocol. The inherent advantage and mechanism of reordering approaches are discussed and then revealed by comparing the coherent area generated by these reordered patterns. The TV order and TW order Hadamard basis patterns can be deterministically described mathematically and easily constructed. Meanwhile, it results in a significant improvement both in the compression ratio and image reconstruction quality. Finally, the realization this protocol in real SPI system in the future will bring the real-time SPI closer to practical applications.

INDEX TERMS Single-pixel imaging, Hadamard basis, total variation, wavelet transform, Fourier domain regularization.

I. INTRODUCTION

Single pixel imaging (SPI) technology, which enables to build compact, low-cost and fast imaging devices, has drawn more research attentions [1], [2]. It has been widely used in 3D imaging [3], [4], terahertz imaging [5], [6], ghost imaging [7] and video acquisition [8]. A general SPI setup is achieved only by a spatial light modulator (SLM) and a single point detector, which records the inner product of the scenes with specific SLM patterns. The image is reconstructed numerically after a sequence of measurements acquired by a series of SLM patterns. Methods of recovering the images include compressed sensing [9] and basis scan [10], [11].

One of the greatest challenges for SPI is real-time imaging technique [8]. When the hardware performance such as switch rate and modulation speed of SLM and sampling speed of single point detector cannot be improved anymore, the best choice is to reduce the measurements (also called compressive measurement) to improve the imaging speed. Hence, the SLM patterns and reconstruction methods are

The associate editor coordinating the review of this manuscript and approving it for publication was Chao Zuo.

crucial to the design of SPI system. The compressed sensing (CS) theory [12] provides an excellent theoretical framework for image reconstruction. It is based on the random SPL patterns and iterative optimization methods such as l_1-magic algorithm [1], Orthogonal Matching Pursuit (OMP) algorithm [13] and TVAL3 algorithm [14]. These algorithms require the images to satisfy the sparse constraint. However, without prior information of the scene, the sparsity ratio of the image remains unknown. Meanwhile, they are not sufficiently fast to allow real time imaging for a medium sized image due to their iterative process. One solution is to find a fast reconstruction method such as one-step reconstruction algorithms for real-time imaging at an appropriate image reconstruction quality. Fortunately, Czajkowski has proposed the Fourier domain regularization inversion (FDRI) reconstruction [15], [16]. This method can make the reconstruction process simplified to one-step matrix multiplication, resulting in super-fast image reconstruction.

The other method to further reduce the imaging time is to reduce the SLM patterns, i.e., compressive measurement. However, there is a tradeoff between the compression ratio and image resolution. For the general images, one cannot acquire a good image quality when the sampling ratio is below 30% in a practical SPI imaging due to the noises. One promising direction is that better designed SLM patterns can improve the image reconstruction quality at a low sampling ratio. Generally used SLM patters include Gaussian matrix, Bernoulli matrix, DCT matrix [15], Hadamard matrix [17]. For most SPI systems, DMDs are used as the SLM, which are inherently limited to be either on or off, can only project 1s and 0s on the modulator [17]. Consequently, Hadamard matrix is the easiest to construct and implement on hardware without binarization or sacrificing the pattern switch rate [18]. Furthermore, it has been found that using a differential measurement of the Hadamard matrix enhances the signal noise ratio (SNR) because it subtracts background noise [19]. Additionally, a significance-based ordering of the Hadamard basis provides a better reconstruction from fewer measurements [20]. The ''Russian Dolls'' (RD) ordering and ''cake cutting'' (CC) ordering Hadamard basis approaches are proposed [20], [21]. CC order was proved to be able to acquire high quality images with super sub-Nyquist sampling ratio even below 0.2% for 1024×1024 images [21]. However, RD order is difficult to construct and has a limited spatial resolution, and CC order can only be fast constructed from the Walsh ordered Hadamard empirically. One also can resort the normal Hadamard basis in other orders. A natural question one would ask is that how to make the most significant patterns projected firstly and which ordering has the optimal compressive ratio and best image recover quality. Besides, the inherent math and physical mechanism existing reordering methods remains unknown.

In this paper, two novel Hadamard basis sorting method: total variation method and total absolute wavelet decomposition coefficients method are put forward. Combined with FDRI reconstruction method, a deep compressive (very low sampling ratio) and super-fast SPI protocol is achieved which can reconstruct a 128×128 image in a few microsecond at the sampling ratio below 5%. Based on this protocol, the reconstructed images obtained from different reordered Hadamard matrices and Gaussian matrix through three image quality assessment indices are numerically compared to find the optimal sorting order and analyze the inherent physics nature.

The rest of this paper is organized as follows. Section II describes the Hadamard basis, fast reconstruction protocol and the image assessment indices adopted. Section III introduces the different principle of reordering Hadamard basis patterns. Section IV gives the numerical simulation and experimental results. Finally, we discuss the influence factors and analyze the inherent physics nature of reordering indicators in Section V and report our conclusions in Section VI.

II. HADAMARD BASIS AND RECONSTRUCTION PROTOCOL

A. HADAMARD BASIS

Hadamard basis generated from the built-in function of MATLAB is the normal Hadamard matrix, which is a symmetric square matrix with elements ± 1. Let H_n be a Hadamard matrix of order n, then the Hadamard matrix of higher order can be given by the following recursive formula,

$$H_{2n} = \begin{bmatrix} H_n & H_n \\ H_n & -H_n \end{bmatrix} \tag{1}$$

where the $H_1 = [1], H_2 = \begin{bmatrix} 1 & 1 \\ 1 & -1 \end{bmatrix}$. Complementary measurement strategy is used when projecting the Hadamard patterns. The Hadamard matrix can be easily divided into two complementary matrices: a positive and a negative subset, expressed as $H = H^+ - H^-$. Figure 1 illustrates the complementary matrices of Hadamard.

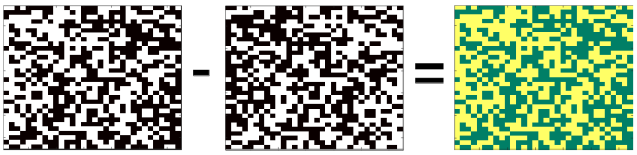

FIGURE 1. Complementary matrices of Hadamard patterns.

B. RECONSTRUCTION PROTOCOL

The reconstruction process of compressive sensing is to solve following ill-posed problem,

$$Y = H \cdot X \tag{2}$$

where Y is measured vector, H is the patterns and X is the object. FDRI algorithm is based on the multiplication of the generalized inverse of rectangular measurement matrix by the measurement vector [15]. For a specific compressed ratio, the measurement matrix and calculation the corresponding pseudoinverse matrix M are calculated and stored

firstly, then the image is recovered by matrix multiplication.

$$X = M \cdot Y \tag{3}$$

The computational time is only the time of one step matrix multiplication. Combined with Hadamard basis patterns, FDRI can be a super-fast reconstruction protocol for SPI. For comparison, we also used the TVAL3 [14] to show the superiority of proposed reconstruction protocol.

C. RECONSTRUCTION ASSESSMENT INDICES

Three different metrics are chosen to quantitatively assess the quality of retrieved images: root mean squared error (RMSE), PSNR, and structural similarity index (SSIM). RMSE is the root-mean-square error between the contaminated reconstruction image and the original image. Assuming I is the original image and K is the reconstructed image, the RMSE is calculated as follow:

$$MSE = \frac{1}{N \times N} \sum_{i=1}^{N} \sum_{j=1}^{N} |I(i,j) - K(i,j)|^2 \tag{4}$$

$$RMSE = \frac{MSE}{\frac{1}{N \times N} \sum_{i}^{N} \sum_{j}^{N} I(i,j)} \tag{5}$$

where N is the size of the images in number of pixels. $I(i,j)$ is the value of the pixel in i_{th} row and j_{th} row in the original distribution, and $K(i,j)$ is the value of the corresponding pixel in the reconstructed image.

PSNR is a full-reference image quality assessment criterion. It is the ratio between the maximum signal power and the noise power. The greater the PSNR value is, the less distorted the reconstruction images will be. In a 2-D imaging process, the PSNR is calculated as follow:

$$PSNR = 10 \times \log_{10}(\frac{Max(I)}{MSE}) \tag{6}$$

SSIM is calculated through mean value, square deviation and covariance of original images and recovered images. Here, the $built - in$ function $ssim$ in MATLAB is used.

III. REORDERING OF HADAMARD BASIS

To achieve deepest compressive sampling ratio, a smallest fraction of most important patterns which can contribute most to the image reconstruction should be projected firstly. Since it is hard to know a priori which patterns can generate the most significant intensity values, one must perform a complete sampling and then pick up the crucial patterns needed according to the recorded signal. Hence, as shown in Figure 2, by using full sampling, the measured signals are sorted in a descending order of absolute value form $|Y|$ for a 128×128 pixels sparse image(Fig.2(a) and Fig.2(c)-(d)) and a natural image (Fig.2(b) and Fig.2(d))), respectively. It is called ''power order'' Hadamard basis.

In this sparse image, all intensities of the white letters and geometries are 0.3, while all values of the black background are 0. According to figure 2, the measured signals of normal order Hadamard are natural distributed. After sorting, few fractions of the corresponding patterns which generate most significant measurements for image reconstruction are used to sample the object. Retrieved images by FDRI at different sampling ratio are shown figure 3. Both sparse image and natural reconstructed by FDRI show a good PSNR at even 5% sampling ratio at ''power order''. For the sampling ratio under 5%, FDRI has a better reconstruction for the natural image than the sparse image. Table 1 shows the comparison of reconstruction results of the natural image by TVAL3 and FDRI. FDRI performs much better in reconstruction time, using just a few microseconds, while the TVAL3 use tens of seconds and more. What's more, these 3 indices confirm that FDRI has a good performance in super-fast image reconstruction quality using Hadamard basis patterns.

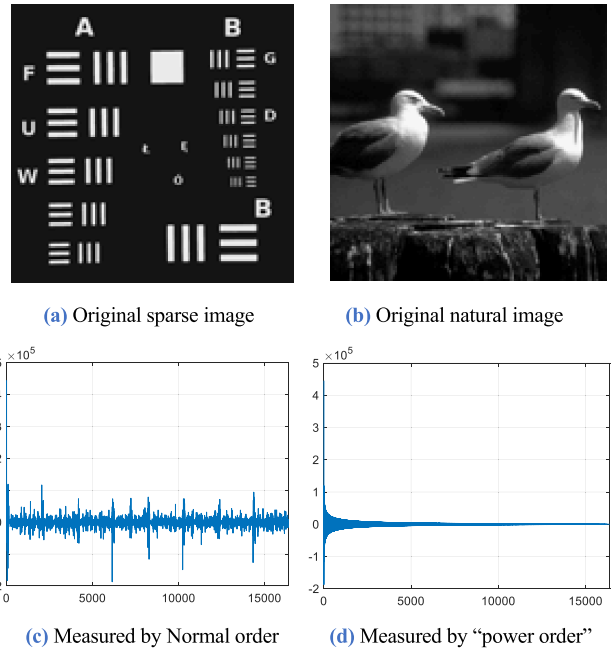

(a) Original sparse image (b) Original natural image

(c) Measured by Normal order (d) Measured by "power order"

FIGURE 2. Original images and measured signal by normal order and "power order" Hadamard basis.

TABLE 1. Comparison of reconstruction results of TVAL3 and FDRI.

Sampling ratio	PSNR		RMSE		SSIM	
	TVAL3	FDRI	TVAL3	FDRI	TVAL3	FDRI
1%	19.77	20.53	0.38	0.36	0.25	0.26
3%	24.25	24.73	0.23	0.21	0.40	0.43
5%	25.57	25.83	0.19	0.19	0.48	0.47
10%	27.41	27.52	0.16	0.16	0.56	0.54
15%	29.06	28.61	0.13	0.13	0.62	0.57

However, for a practical SPI system, it is unlikely to have priori which patterns can generate the most significant values and whether the image is sparse or not, and one cannot measure the signals first and select the most important part. There are many orders for the Hadamard matrix, such

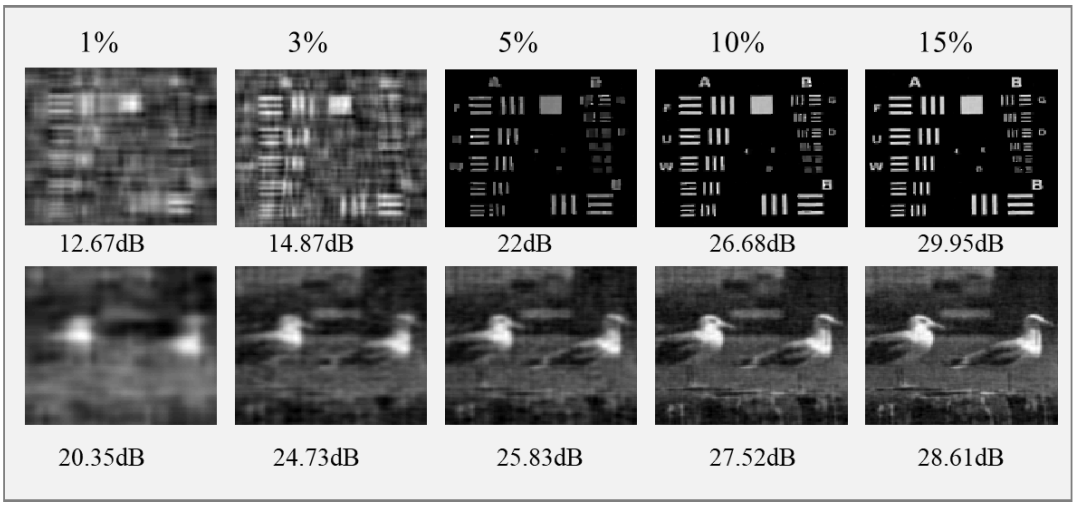

FIGURE 3. Reconstruction of sparse image and natural image by FDRI at different sampling ratio (number below the image is PSNR).

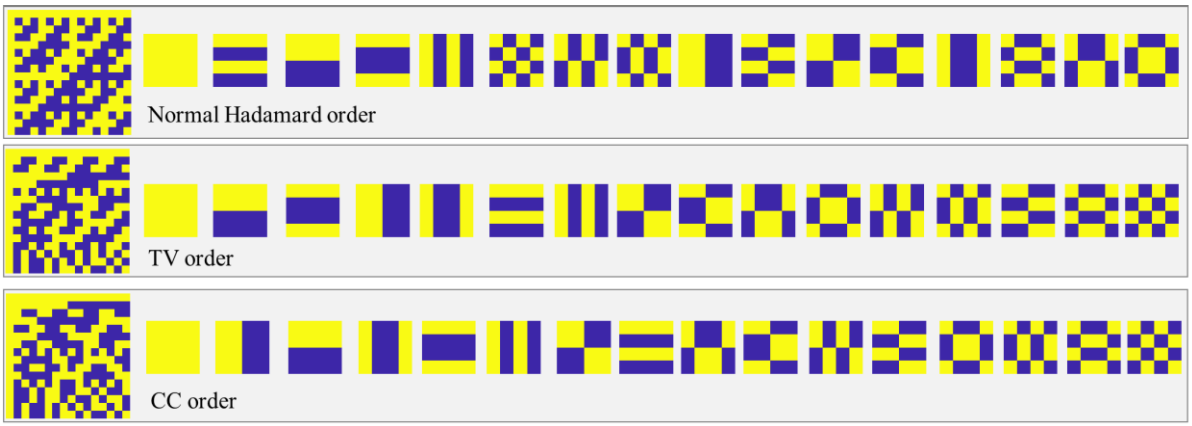

FIGURE 4. Example of reordering the 16 × 16 Hadamard matrix.

as sequence order, dyadic order, Paley-I order, and so on. But none of them can make the important patterns appear first until the "RD" and "CC" order are proposed. The "RD" order is very complicated and difficult to construct. CC order is proposed by Wenkai-Yu which generates an optimized sort of the Hadamard basis. It takes each reshaped basis patterns as a piece of cake and resorting these patterns by their counting their connected regions. The "CC" order is fast calculated and achieved empirically from the Walsh-Hadamard matrix by regularity [21]. Inspired by these methods, we proposed another two different reordering methods: total variation (TV) ascending order (TV order), wavelet coefficients ascending order (TW order), and add another reordering methods into the global comparison: total discrete Fourier transform coefficients ascending order (FFT order) and total discrete Fourier transform coefficients ascending order (DCT order).

A. TOTAL VARIATION ASCENDING ORDER

Total variation is the sum of vertical and horizontal variation of each row of a normal order Hadamard matrix. For a $N \times N$ Hadamard matrix, its total variation of each row is calculated as follows,

$$TV_i = \sum \sqrt{(h_i D_x)^2 + (h_i D_y)^2} \tag{7}$$

where D_x and D_y is the discretized variation operators for the variation in x direction and y direction respectively, which are $N \times N$ sparse diagonal matrices and its elements are 0, -1 and 1; h_{i} is the i_{th} row of normal Hamdard matrix; TV_i is the sum of variations. Firstly, we generate a normal order Hadamard matrix and calculate its total variation of each row, then reorder the rows by their total variation in descending order, which is called TV order. Figure 4 gives an example of 16 × 16 Hadamard basis patterns to illustrate how our TV order and CC order works. The first line includes a 16 × 16 normal order Hadamard matrix and corresponding basis patterns which are 4 × 4 matrices reshaped from each row of the normal order Hadamard matrix. The second and third rows are the TV order and CC order Hadamard matrices and their basis patterns.

B. TOTAL WAVELET COEFFICIENTS ASCENDING ORDER

Wavelet transform can decompose a matrix in multiscale and multiresolution. By choosing a wavelet, we can obtain the wavelet coefficients and then compute each total absolute transformed coefficient, respectively, as shown in equation 8.

$$WL_i = \sum_{1}^{n}\sum_{1}^{n}(ww \cdot M_i \cdot ww') \tag{8}$$

where the ww is wavelet transform matrix, M_i is $n \times n$ matrix reshaped from the i_{th} row of $N\times N$ normal Hamdard matrix, and the i_{th} row is reshaped into a $n \times n$ matrix, where n is the size of the image. WL_i is the sum of wavelet coefficients. Figure 5 shows a 128 × 128 Hadamard basis pattern and its transformed coefficients matrix. The transformed coefficients matrix is a sparse matrix which has lots of zero elements. Then the Hadamard basis is reordered according to its total wavelet coefficients in ascending order. By choosing different wavelet basis, different wavelet orders of Hadamard are obtained. For the sake of simplicity, it is called the ''TW order''.

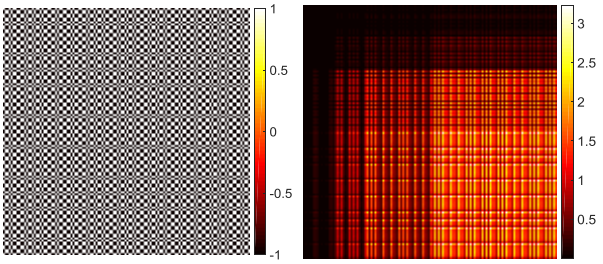

(a) Hadamard basis pattern (b) wavelet transform coefficient matrix

FIGURE 5. One Hadamard basis pattern and its wavelet transform.

C. TOTAL DISCRETE FOURIER AND COSINE TRANSFORM COEFFICIENTS ASCENDING ORDER

Similarly, the FFT order and DCT order is obtained by reordering the Hadamard matrix through their total discrete Fourier transform coefficients and total discrete cosine transform coefficients of each row. Figure 6 illustrates the Fourier transform and cosine transform coefficients of a 128 × 128 Hadamard matrix. Summing up all the coefficients of each Hadamard basis pattern and sorting them in descend order, the FFT order and DCT order are obtained, respectively.

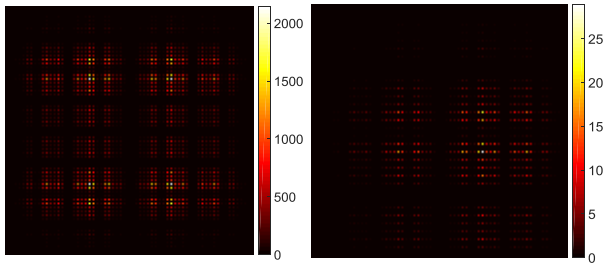

(a) Fourier transform coefficients (b) Cosine transform coefficients

FIGURE 6. Fourier transform and cosine transform coefficients.

IV. SIMULATION RESULTS

A. RECONSTRUCTION OF SPARSE IMAGE

Sparsity of images has great influence on reconstruction in compressed sensing. Imaging spatially sparse objects is not always possible or interesting. Hence, a standard sparse image (Figure2(a)) and a natural image (Figure2(b)) are used to examine the feasibility of proposed protocol.

Although Gaussian random matrix consists of decimals, it is always used in compressed sensing as sampling patterns and has a good performance [22], [23]. Hence, the Gaussian matrix is also added into the comparison for an extensive comparison. The Paley-I type Hadamard matrix is proposed to join the comparison because it has been used in single pixel imaging [24] due to its flexibility in image size. The Paley-I type Hadamard matrix is created by cyclic permutation which is called the Paley order. We choose the Haar wavelet basis for TW order. Figure 6 shows the performance of 6 reordered Hadamard basis, Paley Hadamard matrix and Gaussian random matrix. To quantitatively evaluate the quality of a reconstructed image, the RMSE, PSNR and SSIM of each reconstructed image are calculated as a function of sampling ratio from 1%∼100% at the step of 1%, which is shown in Figures 7(a)-(c). All the simulations are performed on a HP laptop with the RAM of 8 GB and the CPU of Intel Core i7-8550U.

The three indices are computed with the original image as a reference. According to the results, for all the three indices, it is clear that TV order, CC order, Haar order and ''power order'' outperform the Paley order and Gaussian matrix. The FFT order and DCT order cannot get good reconstruction across all the sampling ratio. At the sampling ratio below 5% and above 30%, TV order, Haar order and CC order have best PSNR and RMSE, while the ''power order'' has the best PSNR and RMSE at the sampling ratio between 5% and 30%. For the SSIM, ''power order'' is the best at the sampling ratio under 10% while the TV order, Haar order and CC order almost have the same SSIM. For the SSIM of Haar order, two peaks occur at the sampling ratio of 50% and 75%.

In total, the ''power order'' can provide an optimal reconstruction at the sampling ratio below 10%. TV order can offer near optimal reconstruction and is slightly better than the Haar order and CC order. For deeper compressive SPI, TV order is easy to calculate and is best choice for both reduction of sampling time and reconstruction time.

B. RECONSTRUCTION OF NATURAL IMAGE

Natural images are more common for practical SPI system. To verify the universality of our method, we choose a set of natural images including 49 images [25] and reconstruct these images at sampling ratio from 1%∼100% with a step of 1%. Figure 8(a)-(c) shows the reconstructed results.

Similarly, the proposed reordered Hadamard basis has an overwhelming superiority for any sampling ratio and exceed the Gaussian matrix and Paley order. For the sampling ratio

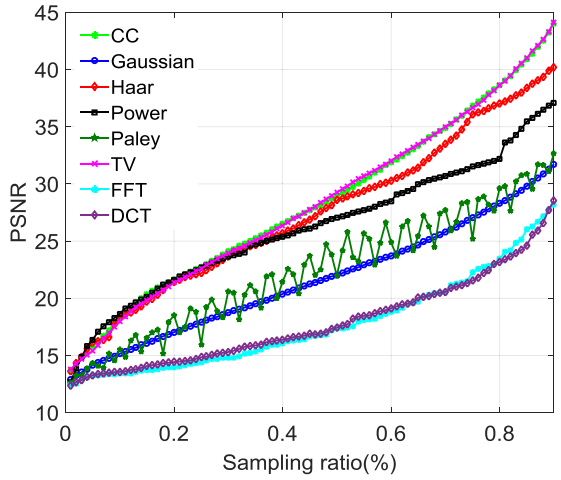

(a) PSNR of reconstructed image by different order

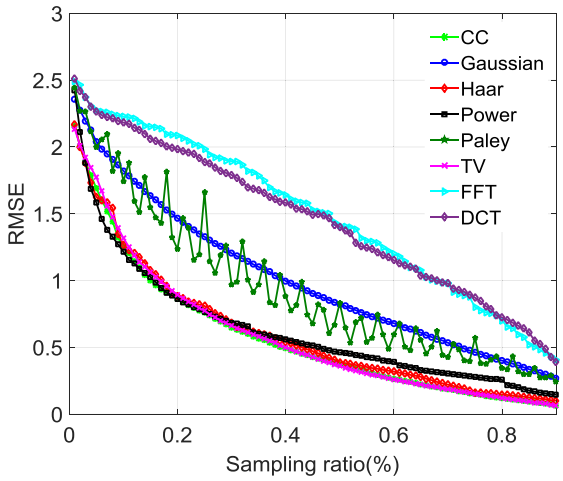

(b) RMSE of reconstructed image by different order

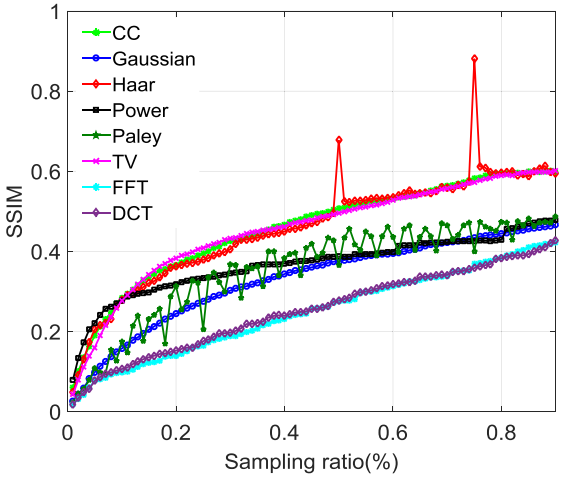

(c) SSIM of reconstructed image by different order

FIGURE 7. Comparison of recovered sparse image quality of the proposed reordering Hadamard basis.

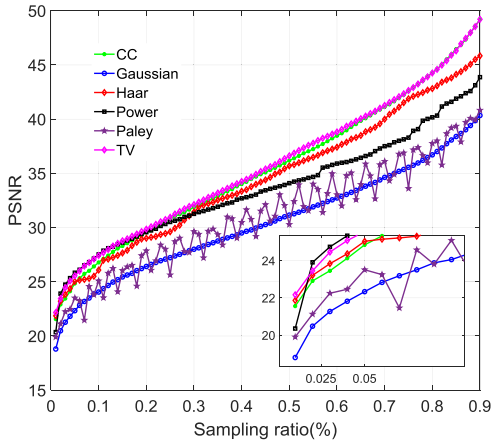

(a) PSNR of different order

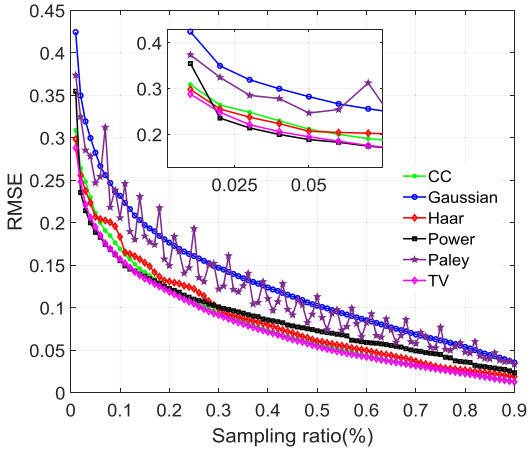

(b) RMSE of different order

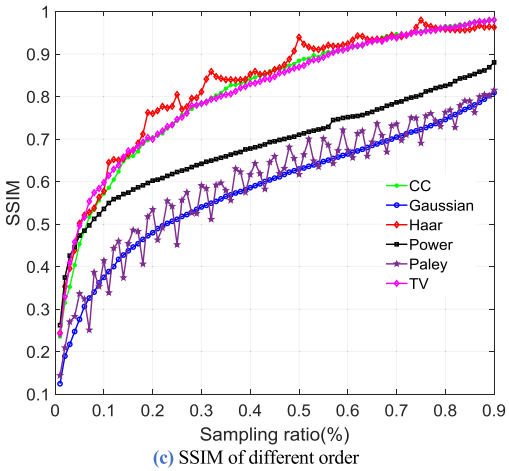

(c) SSIM of different order

FIGURE 8. Comparison of recovered natural image quality of the proposed reordering Hadamard basis.

from 1% to 100%, TV order and CC order have best PSNR, RMSE and SSIM comprehensively. And TV order is slightly better than CC order. For SSIM, Haar order is the best at some points. For visual comparison, figure 9 gives an example of the reconstructed image using 5 different Hadamard matrices at the sampling ratio between 5%∼30%. The Power order and TV order are better than others at the sampling ratio under 15%. The TW order is slightly better than CC order at the sampling ratio under 10%.

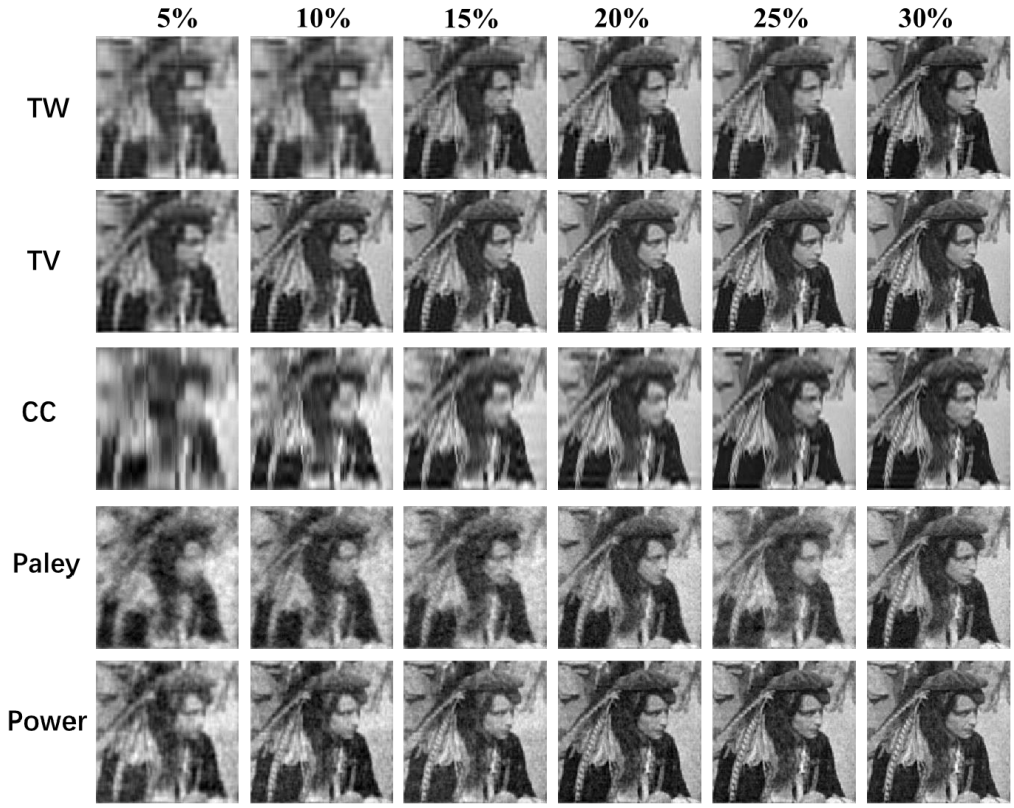

FIGURE 9. Comparison of recovered natural images by 5 different Hadamard matrices.

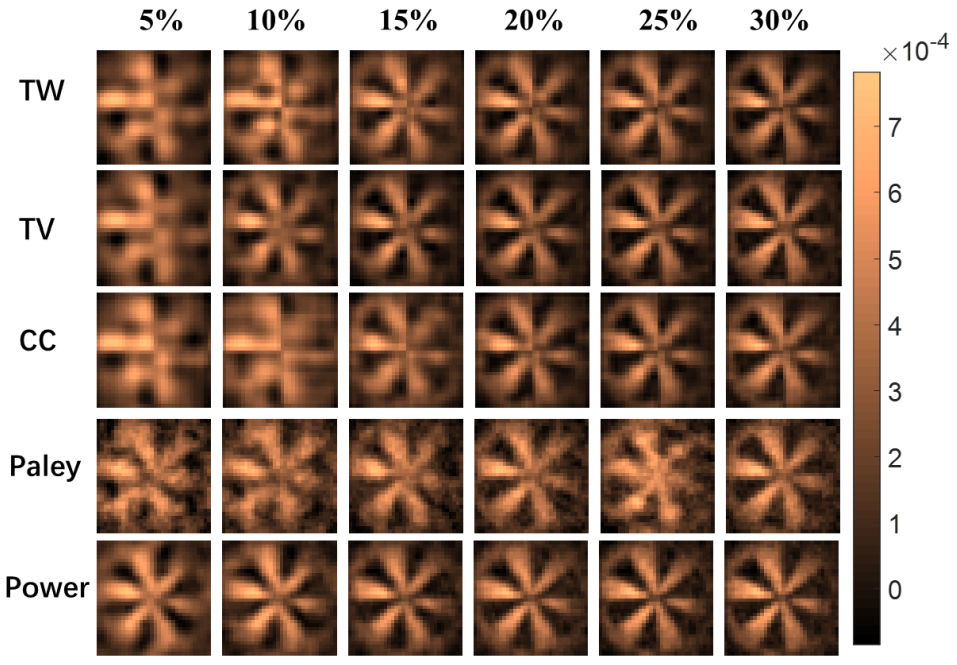

FIGURE 10. Comparison of recovered experimental target images by 5 different Hadamard matrices.

C. EXPERIMENTAL VERIFICATION

The compressive terahertz near-field imaging is used to verify the proposed protocol. Imaging system setup and experimental details can be seen in [26]. The experimental target is a metal wheel. The reconstructed images from measured signals using 5 Hadamard matrices are shown in figure 10. The reconstruction time is only 0.001s at the sampling ratio of 10%. It can be clearly seen that the power order is the best,

and TW order and TV order is better than the CC order and Paley order. For normal Walsh-Hadamard matrices, at least 30% sampling ratio is needed in a practical imaging system, while the proposed TV order and TW order can recover the image under 10% sampling ratio. Hence, the propose protocol can save a lot of time, achieving near real-time terahertz imaging.

V. DISCUSSIONS

A. INFLUENCE OF DIFFERENT WAVELETS

There are a large number of wavelets which are called wavelet family. Different wavelets may result in different TW order and different reconstruction results. Three commonly used wavelets, Haar wavelet, db2 wavelet and sym8 wavelet, are compared. Figure 11(a-c) demonstrates the performance of the three wavelets.

TV order is still better than wavelets order, and Haar wavelet has the near TV order performance for all sampling ratio. At some points, the SSIM of Haar wavelet order is better than TV order. Definitely, Haar wavelet order is better than the db2 wavelet and sym8 wavelet. From mathematic aspect, Hadamard basis patterns are transformed into wavelet domain which a large number of the wavelet coefficients are close to zero also called the sparsity of the patterns. Hence, the total absolute wavelet coefficients are related to the sparsity of the patterns. The sparser the patter is, the smaller total absolute value is. As a result, it will rank in the front of the reordered Hadamard basis. But this mechanism cannot account for the FFT order and DCT order.

B. INFLUENCE OF NOISE

Noise is unavoidable in real imaging systems especially when the signals are weak. It is worthwhile to further compare the reorder techniques in terms of robustness to noise to evaluate their practical application in real imaging system. A random noise which average amplitude is some proportion of the measured signals is added to the measured signals. Figure 12 shows the natural image reconstruction comparison with different noise level, where the x axis represents proportion of amplitude of noise compared the average measured signals. We only compared the TV order, CC order, Haar order and Gaussian matrix.

According to the results, all 3 reorder approaches are robust to noise, and work better than Gaussian matrix.TV order approach perform better than the other two.

C. ANALYSIS OF REORDERING MECHANISM

As mentioned above, total variation of Hadamard matrix, total absolute wavelet decomposition coefficient of basis patterns, and the number of connected regions of basis patterns are used to reorder the Hadamard basis for TV order, wavelet order and CC order. Measured signals from four orders Hadamard basis patterns are shown in figure 13, which just shows the 10-3000 points. The measured intensity from

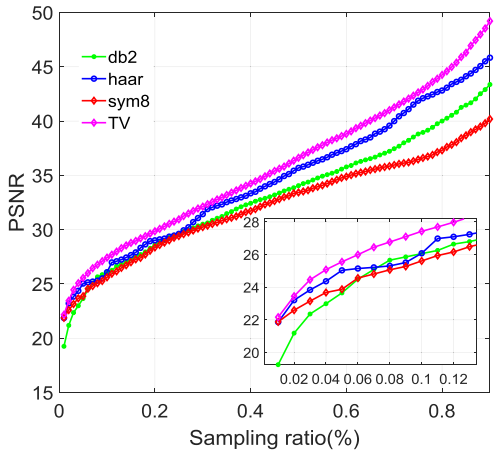

(a) PSNR of different wavelets

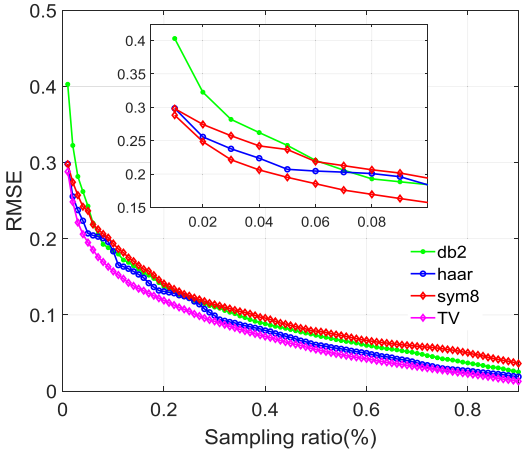

(b) RMSEof different wavelets

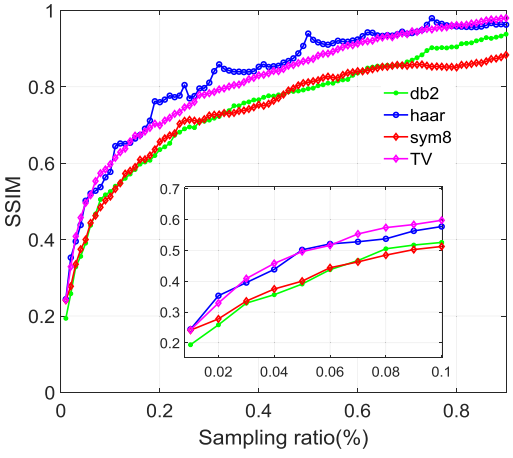

(c) SSIM of different wavelets

FIGURE 11. Comparison of recovered natural image quality of different wavelets.

different orders display similar downtrend but with clear different distribution characteristics.

In compressive theory, the restricted isometry property (RIP), which is described below, can be used to guide the

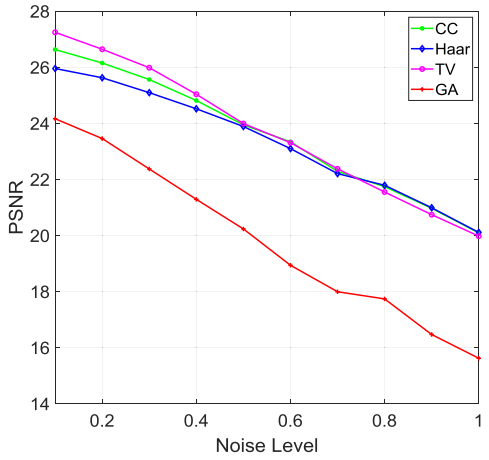

(a) PSNR at differetn noise level

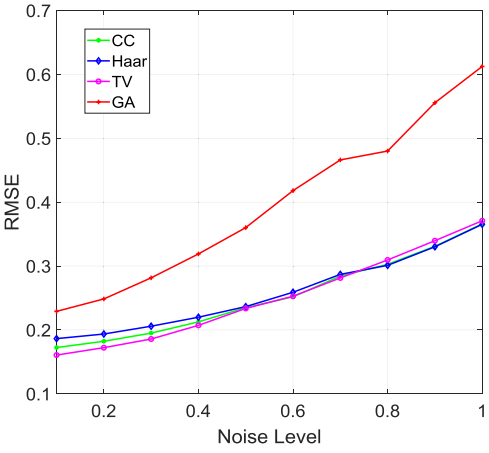

(b) RMSE at differetn noise level

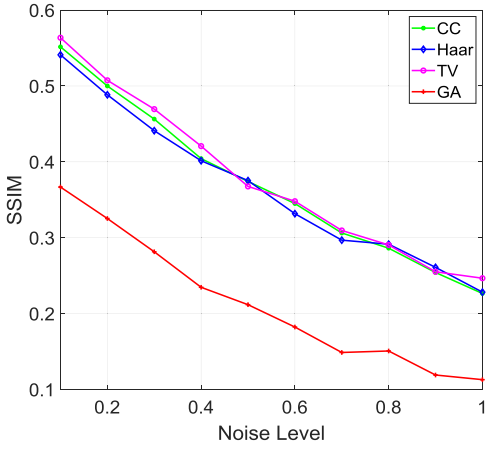

(c) SSIM at differetn noise level

FIGURE 12. Natural image reconstruction comparison with different noise level.

design of sensing matrix.

$$1 - \varepsilon \leq \frac{||Av||_2^2}{||v||_2^2} \leq 1 + \varepsilon \tag{9}$$

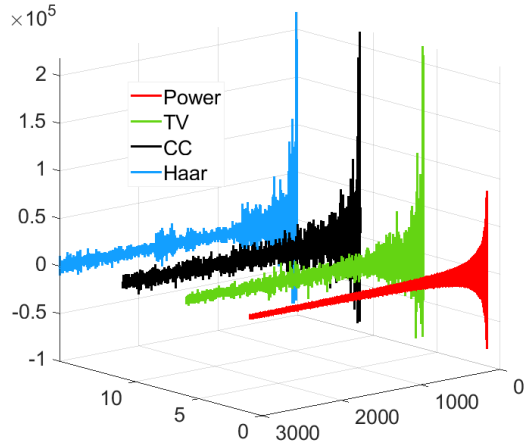

FIGURE 13. Measured signals by different reordered Hadamard basis patterns.

where the $\boldsymbol{A}$ is the measurement matrix, $\boldsymbol{v}$ is the object vector, ε is a small constant. The RIP is used to judge the measurement matrix whether it can recover the object signal or not. The term $||Av||_2$ is the two norm of measured intensities, which has the same distribution of the $|y|$ used in figure 2. The absolute value of measured signals utilizing these proposed Hadamard matrices are replotted in figure 14. From this figure, similar to the figure 13, we see that the measured signals still are distributed with different characteristics.

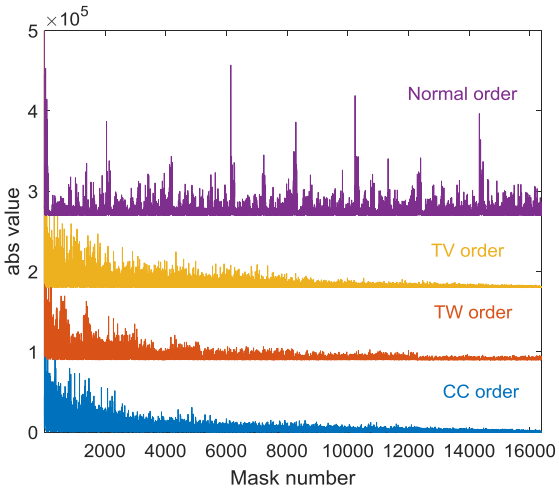

FIGURE 14. Measured signals by proposed matrices.

Apart from analyzing the absolute value of the measurements, the distribution of the eigenvalues of the sensing matrices is also a potential index. We calculated the eigenvalues of the sensing matrices: TV order, CC order, TW order and Normal order, and the distribution of eigenvalues is shown in figure 15.

The eigenvalues of reorder Hadamard matrix are complex and distributed around 128. From this figure, it can be seen that the eigenvalues are distributed with different characteristics. Therefore, it still cannot explain the relationship between

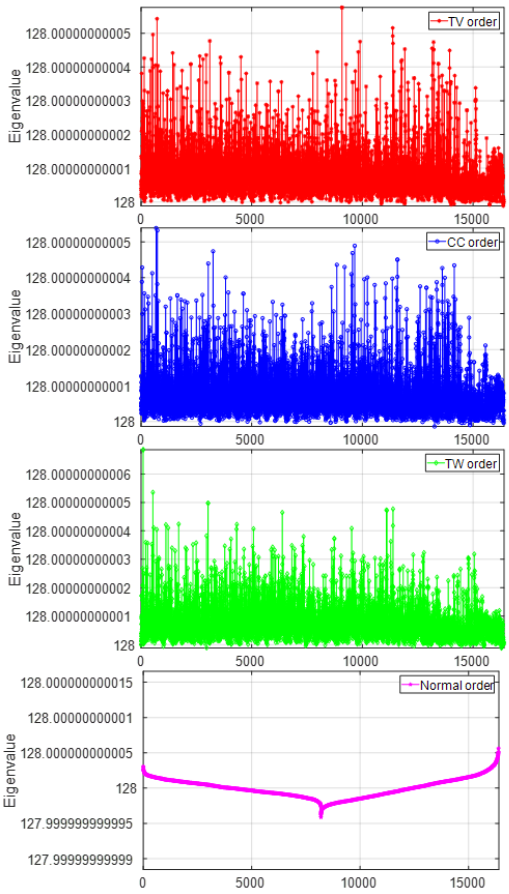

FIGURE 15. Eigenvalues distribution of the sensing matrices.

the proposed methods and other reorder methods using the eigenvalues of sensing matrix.

To further compare the reordering indices, total variations and total absolute wavelet decomposition coefficients of the four reordered Hadamard basis patterns are calculated for the different reordered Hadamard basis patters. Figure 16 and figure 17 shows the normalized total variation and total

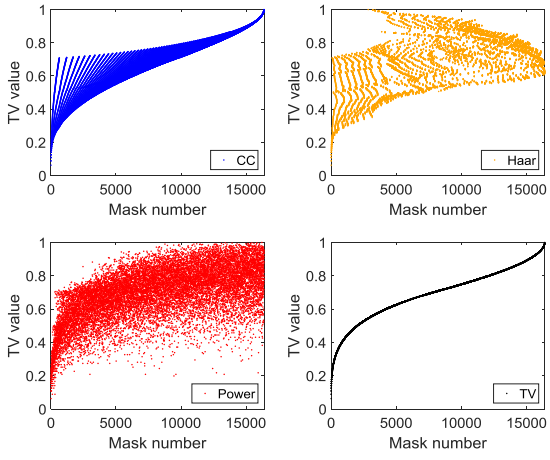

FIGURE 16. Total variation of the proposed four reordered Hadamard matrices comparison.

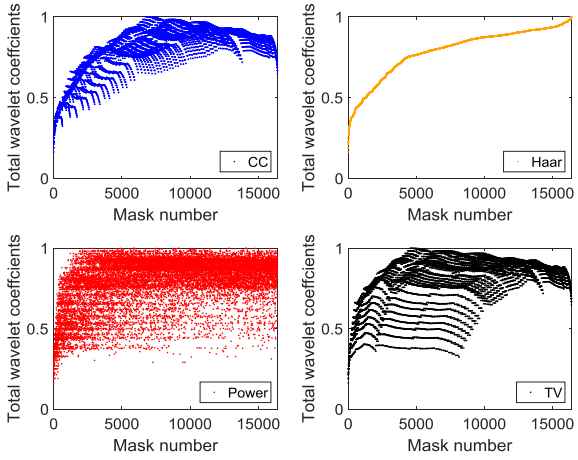

FIGURE 17. Total coefficients of the proposed four reordered Hadamard matrices comparison.

wavelet decomposition coefficients of a 16384 × 16384 reordered Hadamard matrix (H_{128}) in the four orders. In this figure, each point represents the normalized total variation of each row of reordered Hadamard matrix. All the total variations and total wavelet decomposition coefficients have an overall rising trend between 0 and 1. For total variation, similar to the TV order, the CC order has a smoother shape, while Haar order and "power order" have another rising trend which has some violent fluctuations during the rising process. Same with the total variation, total absolute wavelet decomposition coefficients (figure 17) also have the rising trend. But the CC order has the most similarity to the Haar order.

From the viewpoint of mathematic and physical, the complementary Hadamard patterns only consist of 0 and 1, if adjacent elements have different values, it will contribute to the increase of total variation and the number of connected regions, and the decrease of sparsity in a basis pattern. Figure 18 gives the examples of Hadamard basis patterns with different connected regions. Hence, one pattern, which has the smallest total variation, has the least connected region number as well as the best sparsity in wavelet transform. Consequently, this pattern will rank in the front of the resort Hadamard basis patterns. In a practical system, the area of connected elements which have the same value or called connected region in mathematical topology, will reflect the same modulation light, resulting in a coherence area.

According to the [27], for a specific object, the signal noise ratio (SNR) of reconstruction is correlated with the coherence light area. The relationship is described as follows.

$$SNR \propto \frac{m \cdot A_{coh}}{A_{beam}} \tag{10}$$

where m is measurement times, A_{beam} is the area of illumination beam, A_{coh} is the coherence area. Hence, the bigger the total coherence area is, the more it will contributed to the measured signals and reconstruction. Hence, number of the connected regions of reordered Hadamard matrices accounts

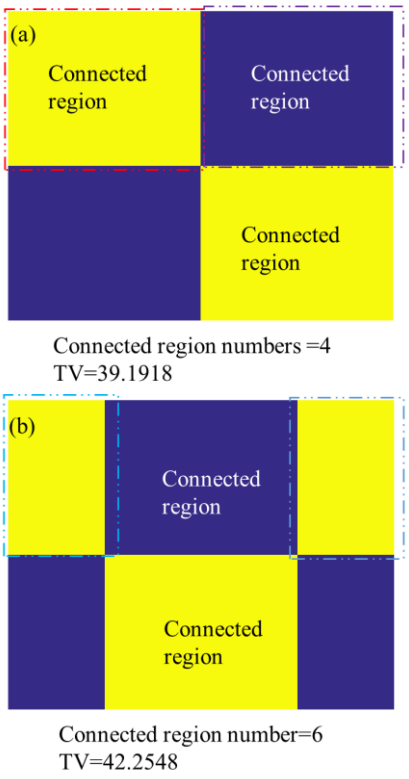

FIGURE 18. Examples of connected region numbers.

for inherent nature mechanism. In a nutshell, all the three reordering approaches, TV order CC order and TW order, can provide almost same reconstruction with the ''power order'' at deep compressive sampling, and even better performance at higher sampling ratio above 30%. TV order and TW order are better than CC order and have clear mathematic and physical mechanism.

VI. SUMMARY AND CONCLUSION

In this paper, we propose a deep compressive and super-fast single pixel imaging protocol based on reordering Hadamard basis patterns and FDRI reconstruction algorithm. This protocol can reconstruct a 128×128 natural image at the sampling ratio of 5% with the PSNR of 25.56dB in 0.00039s, which allows video rate image acquisition. Deep compressive measurement is achieved by using the structured characteristic of Hadamard matrix to reorder the sequences of Hadamard basis patterns. Seven reorder strategies are compared by numerical simulation from sampling ratio of 1%-100%. Results show that the TV order and TW order can be described mathematically and are easy to build, and they can recover the images with the similar image quality of ''power order''. Proposed deep compressive single pixel imaging and super-fast reconstruction are applied to terahertz near-field imaging, achieving near real-time terahertz imaging. The possible mechanisms are discussed and the best core idea and inherent nature of reorder approaches is that it makes the basis patterns which have larger coherence light area modulated first. The TV order and TW order can be deterministically described in mathematics and are the best approaches in terms of computational efficiency and reconstruction performance for any size of images. Finally, the realization of the system hardware in the future will bring the real-time single-pixel imaging closer to practical applications, for example, real-time terahertz single-pixel imaging.

REFERENCES

[1] M. F. Duarte, M. A. Davenport, D. Takhar, J. N. Laska, T. Sun, K. F. Kelly, and R. G. Baraniuk, ''Single-pixel imaging via compressive sampling,'' *IEEE Signal Process. Mag.*, vol. 25, no. 2, pp. 83–91, Mar. 2008.

[2] M. P. Edgar, G. M. Gibson, and M. J. Padgett, ''Principles and prospects for single-pixel imaging,'' *Nature Photon.*, vol. 13, no. 1, pp. 13–20, Jan. 2019.

[3] B. Sun, M. P. Edgar, R. Bowman, L. E. Vittert, S. Welsh, A. Bowman, and M. J. Padgett, ''3D computational imaging with single-pixel detectors,'' *Science*, vol. 340, no. 6134, pp. 844–847, May 2013.

[4] M.-J. Sun, ''Single-pixel three-dimensional imaging with time-based depth resolution,'' *Nature Commun.*, vol. 7, Jul. 2016, Art. no. 12010.

[5] C. M. Watts, D. Shrekenhamer, J. Montoya, G. Lipworth, J. Hunt, T. Sleasman, S. Krishna, D. R. Smith, and W. J. Padilla, ''Terahertz compressive imaging with metamaterial spatial light modulators,'' *Nature Photon.*, vol. 8, no. 8, pp. 605–609, Aug. 2014.

[6] R. I. Stantchev, D. B. Phillips, P. Hobson, S. M. Hornett, M. J. Padgett, and E. Hendry, ''Compressed sensing with near-field THz radiation,'' *Optica*, vol. 4, no. 8, pp. 989–992, Aug. 2017.

[7] W. Chen, ''Ghost identification based on single-pixel imaging in big data environment,'' *Opt. Express*, vol. 25, no. 14, pp. 16509–16516, Jul. 2017.

[8] M. P. Edgar, G. M. Gibson, R. W. Bowman, B. Sun, N. Radwell, K. J. Mitchell, S. S. Welsh, and M. J. Padgett, ''Simultaneous real-time visible and infrared video with single-pixel detectors,'' *Sci. Rep.*, vol. 5, no. 1, Sep. 2015, Art. no. 10669.

[9] M. Rani, S. B. Dhok, and R. B. Deshmukh, ''A systematic review of compressive sensing: Concepts, implementations and applications,'' *IEEE Access*, vol. 6, pp. 4875–4894, 2018.

[10] Z. Zhang, X. Ma, and J. Zhong, ''Single-pixel imaging by means of Fourier spectrum acquisition,'' *Nature Commun.*, vol. 6, no. 1, May 2015, Art. no. 6225.

[11] F. Rousset, N. Ducros, A. Farina, G. Valentini, C. D'Andrea, and F. Peyrin, ''Adaptive basis scan by wavelet prediction for single-pixel imaging,'' *IEEE Trans. Comput. Imag.*, vol. 3, no. 1, pp. 36–46, Mar. 2017.

[12] D. L. Donoho, ''Compressed sensing,'' *IEEE Trans. Inf. Theory*, vol. 52, no. 4, pp. 1289–1306, Apr. 2006.

[13] J. A. Tropp and A. C. Gilbert, ''Signal recovery from random measurements via orthogonal matching pursuit,'' *IEEE Trans. Inf. Theory*, vol. 53, no. 12, pp. 4655–4666, Dec. 2007.

[14] C. Li, W. Yin, H. Jiang, and Y. Zhang, ''An efficient augmented Lagrangian method with applications to total variation minimization,'' *Comput. Optim. Appl.*, vol. 56, pp. 507–530, Jul. 2013.

[15] K. M. Czajkowski, A. Pastuszczak, and R. Kotyński, ''Real-time single-pixel video imaging with Fourier domain regularization,'' *Opt. Express*, vol. 26, no. 16, pp. 20009–20022., Aug. 2018.

[16] K. M. Czajkowski, A. Pastuszczak, and R. Kotynski, ''Single-pixel imaging with sampling distributed over simplex vertices,'' 2018, *arXiv:1811.10348*. [Online]. Available: http://arxiv.org/abs/1811.10348

[17] Z. Zhang, X. Wang, G. Zheng, and J. Zhong, ''Hadamard single-pixel imaging versus Fourier single-pixel imaging,'' *Opt. Express*, vol. 25, no. 16, pp. 19619–19639, Aug. 2017.

[18] Z. Zhang, X. Wang, G. Zheng, and J. Zhong, ''Fast Fourier single-pixel imaging via binary illumination,'' *Sci. Rep.*, vol. 7, no. 1, Dec. 2017, Art. no. 12029.

[19] W.-K. Yu, X.-F. Liu, X.-R. Yao, C. Wang, Y. Zhai, and G.-J. Zhai, ''Complementary compressive imaging for the telescopic system,'' *Sci. Rep.*, vol. 4, no. 1, May 2015, Art. no. 5834.

[20] M.-J. Sun, L.-T. Meng, M. P. Edgar, M. J. Padgett, and N. Radwell, ''A russian dolls ordering of the Hadamard basis for compressive single-pixel imaging,'' *Sci. Rep.*, vol. 7, no. 1, Dec. 2017, Art. no. 3464.

[21] W.-K. Yu, ''Super sub-Nyquist single-pixel imaging by means of cake-cutting Hadamard basis sort,'' *Sensors*, vol. 19, no. 19, p. 4122, 2019.

[22] L. Jacques, D. K. Hammond, and J. M. Fadili, "Dequantizing compressed sensing: When oversampling and non-Gaussian constraints combine," *IEEE Trans. Inf. Theory*, vol. 57, no. 1, pp. 559–571, Jan. 2011.
[23] H. Monajemi, S. Jafarpour, M. Gavish, and D. L. Donoho, "Deterministic matrices matching the compressed sensing phase transitions of Gaussian random matrices," *Proc. Nat. Acad. Sci. USA*, vol. 110, no. 4, pp. 1181–1186, Jan. 2013.
[24] R. I. Stantchev, B. Sun, S. M. Hornett, P. A. Hobson, G. M. Gibson, M. J. Padgett, and E. Hendry, "Noninvasive, near-field terahertz imaging of hidden objects using a single-pixel detector," *Sci. Adv.*, vol. 2, no. 6, Jun. 2016, Art. no. e1600190.
[25] *Dataset of Standard* 512 × 512 *Grayscale Test Images*. Accessed: Dec. 20, 2019. [Online]. Available: http://decsai.ugr.es/cvg/CG/base.htm
[26] S.-C. Chen, L.-H. Du, K. Meng, J. Li, Z.-H. Zhai, Q.-W. Shi, Z.-R. Li, and L.-G. Zhu, "Terahertz wave near-field compressive imaging with a spatial resolution of over λ/100," *Opt. Lett.*, vol. 44, no. 1, pp. 21–24, Jan. 2019.
[27] F. Ferri, D. Magatti, L. A. Lugiato, and A. Gatti, "Differential ghost imaging," *Phys. Rev. Lett.*, vol. 104, no. 25, Jun. 2010, Art. no. 253603.

XIAO YU received the bachelor's degree from the School of Electrical Engineering, Chongqing University, China, in 2015, where he is pursuing the Ph.D. degree. He was a Visiting Academic with the University of Warwick, U.K., from 2018 to 2019. His research interests include the single pixel imaging, compressed sensing, and terahertz imaging.

FAN YANG (Member, IEEE) received the Ph.D. degree from Chongqing University, Chongqing, China, in 2008. He joined the Department of Electrical Engineering, Chongqing University, in 2008, as a Lecturer, where he became an Associate Professor two years later. From 2013 to 2014, he was a Postdoctoral Research Fellow with Oklahoma State University, Stillwater, USA. He is currently a Professor and the Vice Dean of the Department of Electrical Engineering, Chongqing University. He has been conducting research in the areas of computational electromagnetic field and computational imaging.

BING GAO received the Ph.D. degree from the School of Electrical Engineering, Chongqing University, Chongqing, China, in 2016. He is currently a Lecturer. His research interests include the reliability of power modules, the multiphysics coupling field calculation, signal processing, and artificial intelligence.

JIA RAN, photograph and biography not available at the time of publication.

XIN HUANG, photograph and biography not available at the time of publication.